Muscle Satellite Cells and Endothelial Cells: Close Neighbors and Privileged Partners $\boxed{D}$

Christo Christov,*†‡§‖ Fabrice Chrétien,*†‡‖¶ Rana Abou-Khalil,*†‡
Guillaume Bassez,*†‡ Grégoire Vallet,*†‡ François-Jérôme Authier,*†‡
Yann Bassaglia,*†‡ Vasily Shinin,¶ Shahragim Tajbakhsh,¶ Bénédicte Chazaud,*†‡
and Romain K. Gherardi*†‡§

*INSERM, Unité 841, IMRB, Team No. 10, Créteil, F-94000, France; †Université Paris XII-Val de Marne, Créteil, F-94000, France; ‡Service d'Histologie, Département de Pathologie, Hôpital Henri Mondor, Assistance Publique-Hôpitaux de Paris, F-94000 Créteil, France; §"PICTURES" Cell and Tissue Imaging Unit of Institut Mondor de Médecine Moléculaire, IFR 10, Créteil, F-94000 France; and ¶"Stem Cells and Development," Department of Developmental Biology, Pasteur Institute, Paris, F-75015 France

Genetically engineered mice (Myf5[nLacZ/+], Myf5[GFP-P/+]) allowing direct muscle satellite cell (SC) visualization indicate that, in addition to being located beneath myofiber basal laminae, SCs are strikingly close to capillaries. After GFP[+] bone marrow transplantation, blood-borne cells occupying SC niches previously depleted by irradiation were similarly detected near vessels, thereby corroborating the anatomical stability of juxtavascular SC niches. Bromodeoxyuridine pulse-chase experiments also localize quiescent and less quiescent SCs near vessels. SCs, and to a lesser extent myonuclei, were nonrandomly associated with capillaries in humans. Significantly, they were correlated with capillarization of myofibers, regardless to their type, in normal muscle. They also varied in paradigmatic physiological and pathological situations associated with variations of capillary density, including amyopathic dermatomyositis, a unique condition in which muscle capillary loss occurs without myofiber damage, and in athletes in whom capillaries increase in number. Endothelial cell (EC) cultures specifically enhanced SC growth, through IGF-1, HGF, bFGF, PDGF-BB, and VEGF, and, accordingly, cycling SCs remained mainly juxtavascular. Conversely, differentiating myogenic cells were both proangiogenic in vitro and spatiotemporally associated with neoangiogenesis in muscular dystrophy. Thus, SCs are largely juxtavascular and reciprocally interact with ECs during differentiation to support angio-myogenesis.

INTRODUCTION

Muscle tissue repair is a complex biological process that crucially involves activation of stem cells. Skeletal muscle contains two different stem cell types: 1) myogenic stem cells, so-called satellite cells (SCs), that reside beneath the basal lamina of muscle fibers (Mauro, 1961) and express both NCAM/CD56 and early myogenic cell markers such as M-cadherin, Pax7, and Myf5 (Beauchamp et al., 2000; Seale et al., 2000; Hawke and Garry, 2001; Bischoff and Franzini-Armstrong, 2004) and 2) interstitial multipotent stem cells, which are extralaminal, exhibit fibroblastic morphology and do not express myogenic markers (Asakura et al., 2001; Tamaki et al., 2002). SCs are primarily quiescent in skeletal muscle, can self-renew (Collins et al., 2005) and upon activation, proliferate and further differentiate to become fusion-competent myoblasts and ensure muscle regeneration (Hawke

and Garry, 2001; Bischoff and Franzini-Armstrong, 2004). Interstitial "muscle-derived" stem cells give rise to several lineages after transplantation and in this setting, contribute to synchronized reconstitution of blood vessels (pericytes, smooth muscle cells [SMCs], and endothelial cells), peripheral nerve (Schwann cells), and muscle cells (myofibers and SCs; Tamaki et al., 2005). However, participation of multipotent interstitial stem cells in physiological muscle repair appears to be limited. Instead, it is widely accepted that sublaminal SCs represent the pre-eminent muscle stem cell type used for muscle growth, repair and regeneration (Dhawan and Rando, 2005).

Understanding how stem cell niches are organized in vivo and what interactions their progeny develop with neighboring cell types is a critical issue in stem cell biology (Suda et al., 2005). The sublaminar location of SCs led to their identification, but little is known about the anatomical organization of the surroundings and the constituents of the niche. Moreover, signals that are likely conferred to myogenic cells by either direct contacts with the adjacent myofiber or soluble factors released by neighboring nonmuscle cells, constitute one of the major unexplored areas of SC biology (Dhawan and Rando, 2005). It seems plausible that cell–cell contacts between myofibers and SCs play a role in SC maintenance in a quiescence state (Dhawan and Rando, 2005). Such quiescent stem cells anchored in their niche exhibit a low requirement for growth factors (Suda et al., 2005).

Besides the quiescent stem cell niche, a maturation compartment may exist, involving progenitor cells and supportive stromal cells (Suda *et al.*, 2005). We previously showed that activated SCs crucially interact with macrophages recruited at the site of muscle regeneration and receive mitogenic signals from macrophages, mediated by the sequential release of different soluble factors (Chazaud *et al.*, 2003b). Myoblasts, and to a higher extent myotubes, also receive cell-contact–mediated prosurvival signals from macrophages (Sonnet *et al.*, 2006).

In the present study, we focused on the microvascular bed as another partner of SCs. Endothelial cells and myogenic cells may derive from common progenitors at development stages (Kardon *et al.*, 2002) and vascular endothelial progenitor cells are probably essential for muscle organogenesis (Solursh *et al.*, 1987; Le Grand *et al.*, 2004). Moreover, different types of adult stem/progenitor cells crucially interact with the microvascular bed and the term of vascular niche was coined to define this compartment in the bone marrow (Suda *et al.*, 2005) and the hippocampus (Palmer *et al.*, 2000). In bone marrow, the vascular niche is anatomically distinct from the endosteal niche of quiescent stem cells and is required for proliferation and terminal differentiation of hematopoietic progenitor cells (Suda *et al.*, 2005). In the hippocampus, neural stem cells reside and self renew near fine capillaries, receive endothelial cell (EC) instructive cues and form neurovascular units involved in an intimate combination of neurogenesis and angiogenesis (Palmer *et al.*, 2000, Shen *et al.*, 2004). In both cases, stem/progenitor cells were shown to secrete and respond to angiogenic factors (Tordjman *et al.*, 2001; Maurer *et al.*, 2003).

The close association of SCs to microvessels is intriguing (Schmalbruch and Hellhammer, 1977; Chazaud *et al.*, 2003b), but it has been ignored or not acknowledged (Carpenter and Karpati, 2001; Bischoff and Franzini-Armstrong, 2004). In the present study, we documented this association using genetically engineered mice allowing SC visualization and two methods conventionally used to mark stem cell niches in vivo (Lie and Xie, 2005), including bone marrow transplantation and label retention studies. Furthermore, we examined human muscle at steady state and in paradigmatic situations of microvascular loss or increase, to assess the interdependence of SCs and capillaries. Finally, coculture experiments, angiogenesis tests, protein and mRNA array–based detection of growth factors, and functional tests with blocking antibodies allowed us to establish that endothelial cells specifically enhance satellite cell growth and that, in turn, differentiating myogenic cells are proangiogenic.

These findings suggest that quiescent satellite cells, tightly associated with the myofiber in their sublaminal niche, are prepositioned near capillaries and can, therefore, easily interplay with endothelial cells upon activation to set up coordinated angio-myogenesis in a functional manner.

MATERIALS AND METHODS

Transgenic Mouse Strains

Mice Models Allowing Visualization of Satellite Cells. Constructions of both $Myf5^{nlacZ}$ and $Myf5^{GFP-P}$ knock-in mice have been described (Tajbakhsh *et al.*, 1996; Kassar-Duchossoy *et al.*, 2004). Both mice have a ScaI-BstYI deletion in exon 1 (122 amino acids) of the $Myf5$ gene, thus lacking the basic-HLH domain required for $Myf5$ transcription factor activity, and a reporter gene targeted to this exon. $Myf5^{GFP-P/GFP-P}$ are reduced in size, whereas both heterozygote mice, $Myf5^{nlacZ/+}$ and $Myf5^{GFP-P/+}$, are phenotypically normal and were used for the experiments.

Mice Used for Bone Marrow (BM) Transplantation. C57BL/6 mice were transplanted with BM-derived cells from Tg:CAG-green fluorescent protein (GFP) transgenic mice (C57BL/6 TgN[actEGFP]Osb YO1) in which the GFP transgene is expressed under the control of a non-tissue–specific promoter, chicken β-actin with cytomegalovirus enhancer, as a cytoplasmic protein (Okabe *et al.*, 1997).

Animal Experiments

Mouse Handling. All mice were housed in our level 2 biosafety animal facility and received food and water ad libitum. Before manipulations, animals were anesthetized using intraperitoneal injection of chloral hydrate. This study was conducted in accordance with the European Community guidelines for animal care (Journal Officiel des Communautés Européennes, L358, December 18, 1986).

BM Transplantation. Briefly, donor BM cells were obtained by flushing femurs of Tg:CAG-GFP mice with DMEM medium (Invitrogen, Paisley, United Kingdom) and washed twice in cold PBS. Retro-orbital injection of 3×10^7 BM cells in 0.1 ml mouse serum and PBS (1:1) was done in 9.0 Gy-irradiated, 4-wk-old B6 mice (^{60}Co γ rays within 1 d before BM transplantation) as previously reported (Dreyfus *et al.*, 2004). After transplantation, mice received 10 mg/kg/d ciprofloxacin for 10 d to prevent infection during the aplastic phase. Blood chimerism >95% was controlled by flow cytometry 4 wk after transplantation and tibialis anterior (TA) muscles were examined 6 mo after transplantation.

Bromodeoxyuridine (BrdU) Pulse-Chase Experiments. $Myf5^{nlacZ/+}$ pups received 50 mg/kg BrdU diluted in 20 μl PBS by ip route twice daily from postnatal days 3–8. After a chase period of 6 wk, mice were killed and TA muscles were examined by β-Gal BrdU retention in β-Gal$^+$ satellite cell nuclei. As a control, one $Myf5^{nlacZ/+}$ mouse from the series received a notexin injection (25 μg/ml in 10 μl PBS) in TA muscle 6 wk after exposure and had the injected TA examined 2 wk later to assess dilution of BrdU in the progeny of the previously quiescent satellite cells.

Muscle Samples

Normal muscle samples were obtained in 20 human adults (aged from 24 to 73 y, from various muscle groups, including 12 deltoid, 4 vastus lateralis, 2 gastrocnemius, and 2 peroneus brevis muscles), in 3 adult C57/B6 mice (TA muscle), in 2 adult retriever dogs (sartorius muscle) and, for electron microscopy, in 10 adult Wistar rats (extensor digitorum longus muscle). Muscle samples also collected from deltoid muscle of 3 heavy-training athletes who had no significant myopathologic alterations (males aged from 32 to 39 y practicing intense daily push-up training), of 3 patients with amyopathic dermatomyositis (aDM) collected from a previous study (Cosnes *et al.*, 1995; 2 females, 1 male aged from 32 to 39 y), and of 3 boys with Duchenne muscular dystrophy (DMD; males aged from 2 to 14 y). Muscle samples were frozen and kept at -80°C before processing.

Immunohistochemistry

In mouse tissues, vessels were immunostained using anti-laminin 1 (1:50, polyclonal, DakoCytomation, Glostrup, Denmark) or anti-collagen IV (1:50, polyclonal, Chemicon, Temecula, CA) antibodies revealed by Cy3-conjugated secondary antibodies (Jackson ImmunoResearch Laboratories, West Grove, PA). Because of HCl pretreatment required for BrdU immunohistochemistry, we combined chromogenic and fluorescence revelation approaches on the same preparation. First, endogenous alkaline phosphatase activity of microvascular cells (Pearce *et al.*, 2000) was detected using fast red (forming both chromogenic and fluorescent red precipitate) followed by chromogenic immunohistochemistry against β-galactosidase (β-Gal; using a polyclonal domestic antibody, from Pasteur Institute, 1:2000 revealed by a peroxidase-conjugated secondary antibody) forming a brown precipitate. Afterward, sections were treated with 2 N HCl for 30 min at 37°C, and BrdU was detected using a sheep polyclonal antibody (1:200, Abcam, Cambridge, MA) revealed by FITC-conjugated secondary antibody (Jackson ImmunoResearch Laboratories).

In human tissues, several antibodies were used alone or in combination to localize and identify SCs and their progeny, ECs and vascular endothelial growth factor (VEGF). They included antibodies against laminin-1 (1:500, ref L9393, Sigma Aldrich, St-Louis, MO) for basal laminae, MYF5 (1:50, ref sc302, Santa Cruz Biotechnology, Santa Cruz, CA) for undifferentiated SCs, CD56/NCAM (1:100, ref PN6602705, Beckman Coulter, Fullerton, CA) for both quiescent and differentiating myogenic cells, myogenin (1:200, ref M3559, DakoCytomation) for differentiating myogenic cells, CD31 (1:50, ref M0823, DakoCytomation) and von Willebrand factor (vWF; 1:500, ref A0082, DakoCytomation) for ECs, Ki-67 antigen (1:50, ref M7240, DakoCytomation) for cycling cells, and VEGF (1:100, AF293NA, R&D Systems, Minneapolis, MN, for immunofluorescence; or 1:50, sc-152, Santa Cruz Biotechnology, with SuperPicTure polymer detection kit, Zymed, South San Francisco, CA; and AEC as a chromogen for light microscopy). Dogs samples were labeled using the same antibodies to CD56/NCAM and vWF.

Electron and Confocal Microscopy

Transmission electron microscopy was performed after conventional processing of muscle samples using a Philips-410 microscope (Mahwah, NJ). Confocal microscopy (Zeiss LSM 410 and a ×63 PlanApo NA 1.4 oil objective, Carl Zeiss, Oberkochen, Germany) on 10–30-μm-thick sections and deconvolution of stacks of optical sections obtained along the Z-axis were used to obtain high-resolution images and three-dimensional (3D) volume reconstructions. Steps along the optical axis were set at 0.2–0.3 μm and pixel size in X,Y at 0.11–0.14 μm, thus respecting Nyqvist's criteria optimal for subsequent deconvolution. Z-stacks acquired separately for each channel (green or red) were subjected to iterative optical deconvolution by the AxioVision 4.2 software package defining appropriate parameters of a theoretical Point Spread Function and settings to correct for optical aberration. Deconvolution (15–25 iterations) was performed on a personal computer equipped with a Pentium 4 processor (3.0 GHz, 2 Go RAM). In rare cases, better results were obtained by the Nearest Neighbor algorithm of AxioVision 4.2. 3D reconstructions combining both channels were then obtained in the transparency option of the 4D module of AxioVision 4.2. Measurement of the minimal distance between SC and the neighboring capillary were carried out on the projection (rotation) that excluded spurious colocalization of channels that could potentially result from the considerable Z-thickness of the reconstruction (10–20 μm).

Morphometric Data Collection

Muscle areas showing motor endplates were excluded from analysis. Immunostained sections were digitized with a Hamamatsu CDD device (Hamamatsu Photonics KK, Hamamatsu, Japan) and subjected to morphometric analysis using different modules of the KS4003.0 (Carl Zeiss) and Simple PCI image analysis software (C-Imaging; Compix, Cranberry Township, PA). Each object (SC, Cap, myonuclei, or VSP) was defined as a point with X and Y coordinates in a study area including at least 1000 myofibers per specimen. Because of either difficulty to discriminate between closely associated structures on double-immunostainings or limited use of antibodies of the same species for double-immunostainings, some quantitative evaluations were conducted using single immunostainings on alternate muscle cross sections. For example, alternate sections were immunostained for MYF5, CD31, and myogenin, myogenic cell positions being manually reported in the graphic plane of image reconstruction of the alternate immunostaining of capillaries.

Univariate Spatial Point Pattern Analysis

To explore if point distributions deviate from complete spatial randomness (CSR), we calculated spatial point pattern statistics with the ADE4 software package, using Ripley's K-function for univariate point patterns, and both the Kr function and a quadrat test for bivariate patterns (Ripley, 1988). Basically, the K function assesses for each point the cumulative number of neighboring points within increments of a predefined distance t compared with the expected number of neighbors under the null hypothesis of CSR. These increments define "n" concentric rings so that the outer radius of the external ring r = nt. According to recommendations of the ADE4 manual, t and n values were determined for each set of data, taking into account both size of the study area R and the observed minimal distances between points. The definition of Ripley's K is K(r) = N(r)/λ, where N(r) is the number of neighbors within distance r and λ is the intensity of the pattern. Under CSR, K(r) = πr2, in case of clustering, K(r) > πr2, and in case of regularity, K(r) <πr2. By convention, K(r) is substituted by L(r) [L(r) = $\sqrt{K(r)/\pi}$ − t], this transformation offering the advantage of L(r) = 0 under CSR, L(r) >0 for clustered, and L(r) <0 for regular patterns. Edge correction was carried out as proposed by Ripley (Ripley, 1988). Deviation from CSR was tested by plotting L(r) values against the envelope of significance at p < 0.0001 for the null hypothesis of CSR. This envelope was built using the Monte Carlo method that consists in the realization of 9999 CSR patterns of the same intensity as the observed pattern. Graphically, values above the upper limit of the envelope indicate clustering, whereas values below its lower limit indicate regularity.

Bivariate Point Pattern Analysis

The Kr function, and its Lr transformation, for bivariate patterns is identical to Ripleys' K with the exception that points on which the function is centered and neighbor points are of two different types, i.e., correspond to different objects. Graphic expression of results was similar to that used for Ripleys' K. The distribution of real objects, such as SC and myonuclei, relative to capillaries was compared with that of randomly distributed virtual sarcolemmal points (VSP), one object per myofiber being randomly inserted following a clock dial scheme.

Quadrat Test

A quadrat test grid was superimposed in the graphic plane of each image. The grid square size (21 μm diagonally, 225 μm2) was chosen to enclose the largest clusters of points detected by bivariate analysis, as deduced from the graphic expression of the K function. Each square was examined for the presence of SC, myonuclei, VSP and Cap, and colocalization was estimated by a Fisher's exact test comparing the relative number of squares containing a capillary and either SC, myonuclei, or VSP. In some tests, the capillary area (μm2) in each square was measured after color segmentation (DAB, brown) of CD31 labeling of vessels using KS400 3.0.

Myofiber Capillarization Evaluation

Muscle fiber capillarization in normal, amyopathic dermatomyositis (aDM) and athlete muscles was assessed by the number of capillaries bordering each individual fiber, as previously described (Emslie-Smith and Engel, 1990). Cap numbers and frequency distribution in aDM and control patients of our study were closely similar to those previously reported (Emslie-Smith and Engel, 1990).

Cell Cultures

Unless indicated, culture media components were from Invitrogen (Paisley) and culture plastics from TPP (Trasadingen, Switzerland). Human myogenic precursor cells (mpc) were cultured from muscle samples as previously described (Chazaud et al., 2003b). mpc were grown in HAM-F12 medium containing 15% fetal calf serum (FCS). Only cultures presenting over 95% NCAM/CD56$^+$ (1/20, 123C3, Sanbio/Monosan, Uden, Netherlands) cells were used. mpc differentiation was assessed by myogenin immunoblotting. The MRC-5 human fibroblastic cell line was obtained from ATCC (LGC-Promochem, Molsheim, France) and cultured in MEM containing 10% FCS and 1% NEAA. human umbilical vascular ECs (HUVECs) and human microvascular ECs (HMECs) were obtained from Promocell (Heidelberg, Germany) and cultured in EC growth medium (Promocell). SMCs were obtained from human pulmonary arteries kindly provided by Dr. S. Eddahibi (INSERM U651, Créteil, France) and cultured in RPMI containing 10% FCS and 1% NEAA.

In Vitro Angiogenesis Assay

HUVECs were seeded (30,000 cells/well) in 24-well tissue culture plates coated with growth factor-reduced Matrigel (0.3 ml/well, BD Biosciences, Franklin Lakes, NJ) that was allowed to solidify at 37°C for 30 min. Cells were incubated in serum-free medium or in 24-h mpc-conditioned medium for 24 h at 37°C. The cells were photographed using an inverted photomicroscope (DMIRB Leica, Leica Microsystems, Wetzlar, Germany) with a CCD camera (CoolSnap, Photometrics, Roper Scientific Tucson, AZ). Tube formation was assessed in five randomly selected ×20 powerfields, using the number of branching points in the network per field and the proportion of connected cells (number of connected cells among the total number of cells in the same field; Jones et al., 1999).

Indirect Cocultures

MRC-5 fibroblasts were seeded at 15,000 cells/cm2 and SMCs and mpc at 20,000 cells/cm2 in Falcon inserts (0.4 μm diameter pores; Falcon, BD Biosciences); EC were seeded at 30,000 cells/cm2 and 3 d after confluence, EC monolayer integrity was assessed in two wells by absence of trypan blue (0.2% in 0.1% bovine serum albumin) translocation from upper to lower chamber after a 3-h incubation. mpc were seeded into 24-well plates at 3000 cells/cm2 and allowed to adhere in their culture medium for 6 h. Then, inserts were placed over the mpc-containing well, and the medium of both chamber was changed for MCDB-131 medium containing 2% FCS and 1.5 μg/ml endothelial cell growth supplement. The medium was changed twice weekly. At each time point, mpc density was determined by counting cells after trypsinization, and the number of cells present in the upper chamber was also evaluated. In these conditions, the number of ECs remains constant at each time point as they form impermeable monolayers. In contrast, the number of SMCs, MRC-5, and control mpc increased during time of experiment to reach approximately 60,000, 60,000, and 40,000 cells/cm2, respectively. To avoid bias due to the different numbers of cells in the upper chamber at each time point, calculation of the effect on mpc growth was normalized to 30,000 cells/cm2, thus allowing comparison of individual cell biological activity, as previously reported (Chazaud et al., 2003b). All these in vitro experiments were performed using at least three different cultures. In some experiments, blocking antibodies were added in the well at saturating concentrations (calculated from IC50): anti-insulin-like growth factor (IGF)-1 (6 μg/ml, AF291NA, R&D), anti-platelet-derived growth factor (PDGF-BB; 5 μg/ml, AF220NA, R&D), anti-basic fibroblast growth factor (bFGF; 6 μg/ml, AF233NA, R&D), anti-hepatocyte growth factor (HGF; 5 μg/ml, AF294NA, R&D), and anti-vascular endothelial growth factor (VEGF; 6 μg/ml, AF293NA, R&D). Controls included addition of whole mice immunoglobulin (Ig) Gs (6 μg/ml, Vector Laboratories, Burlingame, CA), antibodies against muscle membrane protein dysferlin (3 μg/ml, Novocastra Laboratories, Newcastle, United Kingdom), and antibodies against MCP-1 (5 μg/ml, P500-P34, Abcys, Paris, France), a chemokine that is secreted by ECs (Cleaver and Melton, 2003) and the receptor of which is expressed by human mpc (DNA array, data not shown).

mpc grown alone were subjected to similar blocking antibody experiments and to recombinant human VEGF (R&D systems) added at 25 ng/ml.
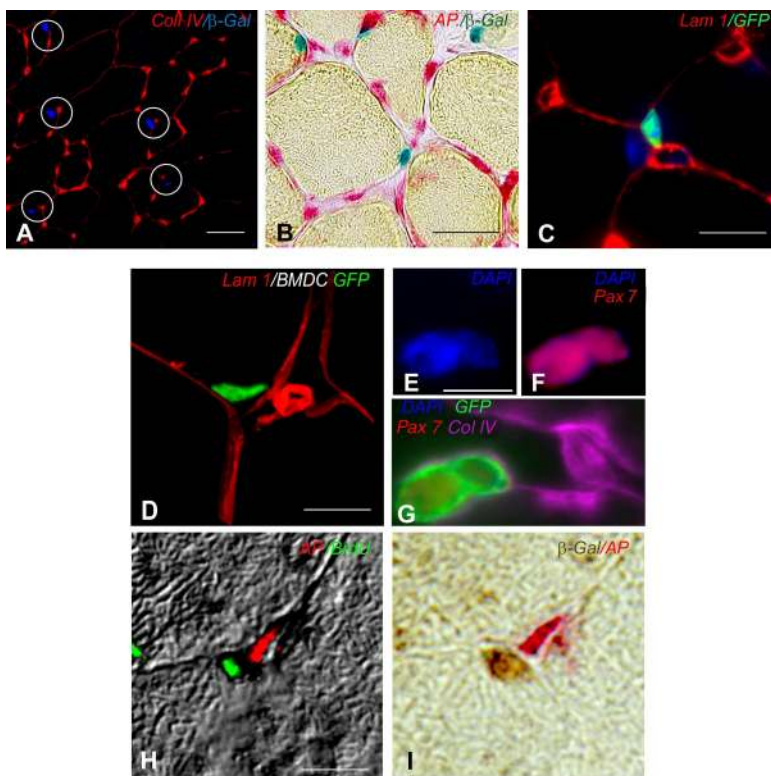
Figure 1. SC proximity to capillaries in mouse models. (A) TA muscle cryosections from $Myf5^{nlacZ/+}$ mouse in which SC nuclei expressing nuclear β-Gal activity (blue pseudocolor) are observed close to microvessels whose thick basal lamina is visualized by enhanced collagen IV immunoreactivity (red); bar, 10 μm. (B) TA muscle cryosections from $Myf5^{nlacZ/+}$ mouse in which most SC nuclei expressing nuclear β-Gal activity (blue) are found close to capillaries expressing alkaline phosphatase activity (red); bar, 10 μm. (C) TA muscle cryosections from $Myf5^{GFP-P/+}$ mouse in which one SC–expressing cytoplasmic GFP (green) is closely associated with a capillary. Laminin 1 is labeled in red. Bar, 10 μm. (D) TA muscle cryosections from a WT mouse transplanted with GFP+ BM-derived cells (BMDC) showing a blood-borne GFP+ cell housed in a juxtavascular SC niche. Bar, 10 μm. (E) The nucleus (blue) that expresses the satellite cell marker Pax7 (red) (F) belongs to a blood-borne GFP+ cell (green) (G). Collagen IV immunostaining (purple) performed as a second step indicates that the cell is sublaminal and juxtavascular (G). (H and I) TA muscle cryosections from a $Myf5^{nlacZ/+}$ mouse perinatally infused with BrdU showing one label-retaining SC located close to a capillary: BrdU immunostaining appears in fluorescent green in both dark field (H) and merge with DIC (H), microvascular alkaline phosphatase activity appears in red at both fluorescent (H) and photonic (I) microscopy; SC nuclear β-Gal antigen is revealed in brown by immunoperoxidase (I). Bar, 10 μm.

DNA Array

Total RNA was prepared from mpc at day 14 of culture using the RNeasy mini kit (Qiagen, Hilden, Germany). All further steps were performed according to the manufacturer's instructions in the human cytokine array kit (R&D Systems). Analysis was performed using Image Quant software (Amersham, Buckinghamshire, United Kingdom), that allows background noise subtraction, correction for the variation of density for housekeeping genes (all genes showed the same intensity variation between the 2 membranes), and finally, densitometric analysis of signals above internal negative controls. Results were expressed in arbitrary units.

Protein Array

Twenty-four-hour HUVEC-conditioned medium was subjected to protein array according to the manufacturer's instructions in RayBio Human Cytokine Antibody Array (RayBiotech, Norcross, GA). Densitometric analysis was performed as described above for DNA array.

Statistical Analyses

Fischer's exact test was used to compare colocalizations in the quadrat test. χ^2 test was used to compare frequency of SCs associated with variously capillarized myofibers and with various Cap types. Student's t test was used in in vitro experiments. $p < 0.05$ was considered significant.

RESULTS

Genetically Engineered Mice Reveal Juxtavascular Location of Most SCs

Neither electron microscopy nor teased fiber preparations are appropriate for the study of the spatial relationships between SCs and capillaries. Because immunocytochemical detection of mouse SCs is suboptimal, we used genetically engineered mice to visualize SCs in TA muscle cryosections. We first used the heterozygous $Myf5^{nlacZ/+}$ mouse, which has a reporter gene encoding nuclear-localizing β-Gal targeted to the *Myf5* locus such that expression of endogenous Myf5 is reported by β-Gal activity, thus allowing detection of SC nuclei (Tajbakhsh *et al.*, 1996; Beauchamp *et al.*, 2000). SCs appeared strikingly associated with capillaries when

β-gal activity revelation was combined with either immunohistochemistry for basal lamina-specific collagen IV (Figure 1A) or histoenzymatic reaction for microvascular alkaline phosphatase activity (Figure 1B). Then we used the $Myf5^{GFP-P/+}$ mouse, which has a reporter gene encoding cytoplasmic GFP targeted to the *Myf5* locus (Kassar-Duchossoy *et al.*, 2004). For unknown reasons, this mouse allows detection of a smaller proportion of SCs than the $Myf5^{nlacZ/+}$ mouse, but offers the advantage of visualizing SC cytoplasmic processes. Cryosections immunostained for laminin 1 showed that the mean distance separating GFP+ SCs (n = 100) from capillaries was 2.6 $\pm$ 3.3 μm : 82% of SCs were at <5 μm from endothelial cells (ECs), 12% at 5–10 μm, and 7% at >10 μm (Figure 1C).

It has been suggested that SCs form an heterogeneous population (Schultz and Lipton 1982; Molnar *et al.*, 1996; Rouger *et al.*, 2004), raising the possibility that SC subpopulations might have different spatial relationships with capillaries, according, for example, to ontogenic or cycling rate specificities. We addressed this point by using two commonly used stem cell niche spotting methods (Li and Xie, 2005) and detection of quiescent stem cells retaining the BrdU label.

Juxtavascular Niches Can Incorporate Bone Marrow–derived Cells

We first tracked bone marrow–derived cells in mice in which stem cell niches are first depleted through irradiation (LaBarge and Blau, 2002). Although sublaminal SCs are derived mainly from somites (Gros *et al.*, 2005), a small numbers of SCs may be generated from bone marrow grafts (LaBarge and Blau, 2002; Dreyfus *et al.*, 2004). These ectopic SCs express canonic SC markers (Dreyfus *et al.*, 2004; Chretien *et al.*, 2005) but exhibit very limited myogenic potential once reisolated from muscle (Sherwood *et al.*, 2004). Thus, they might represent foreign

stem cells squatting in SC niches. If BMT experiments are of unknown significance in terms of SC lineage, they uniquely allow demonstration that, in the absence of the resident SC, the niche may be occupied by another cell. This information is important because adult stem cell niches are currently conceived as specific anatomical stem cell anchoring sites, which are strategically placed in the tissue and stable enough to welcome a novel stem cell (Li and Xie, 2005); this view is opposed to that of a labile microenvironment, freely generated at the stem cell request anywhere in the tissue, strictly dependent on signals from a given stem cell, and thus disappearing with it.

Five 4-wk-old, 9.0-Gy–irradiated, wild C57BL/6 mice were transplanted with 3×10^7 BM-derived cells from Tg:CAG-GFP transgenic mice in which the GFP transgene is expressed under the control of a ubiquitous promoter (Okabe *et al.,* 1997) and serves as an unambiguous marker for donor-derived cells in host tissues (LaBarge and Blau, 2002; Dreyfus *et al.,* 2004). Six months after transplantation, TA muscle transections immunostained for basal lamina markers (laminin or collagen IV) showed a total number of 94 GFP+ cells, 38 of which were sublaminal (Figure 1D). Coimmunostaining showed nuclear Pax7 expression in a proportion of GFP-positive cells (n = 7), as previously reported (Dreyfus *et al.,* 2004; Chretien *et al.,* 2005). Vascular proximity of these cells became obvious when collagen IV immunostaining was done as a supplementary reaction and merged with initial images of Pax7+ and GFP+ cells (Figure 1, E–G).

The mean distance separating sublaminal GFP$^+$ cells from capillaries was 2.2 ± 3.8 μm : 89% were at <5 μm from ECs, 8% at 5–10 μm, and 3% at >10 μm. This result is in keeping with that obtained for SCs from $Myf5^{GFP-P/+}$ mice, suggesting that juxta-vascular SC niches are stable anchoring sites housing stem cells regardless of their origin.

Juxtavascular Niches Contain Slowly Cycling BrdU-retaining SCs

The thymidine analogue BrdU can label newly synthesized DNA in cycling cells. It is assumed that, after a long period of chase, slowly cycling cells retain a concentration of label sufficiently high to allow their detection (Fuchs *et al.,* 2004). To readily discriminate SC nuclei from both myonuclei and interstitial cell nuclei that can also retain BrdU, we used $Myf5^{nlacZ/+}$ mice. BrdU was administered intraperitoneally to 5 mice, twice daily from postnatal day 3 to 8, an age at which ~90% of TA muscle SCs incorporate BrdU (Shinin *et al.,* 2006), presumably because they actively divide to increase muscle mass. Those cells that did not divide subsequently were detected in TA muscle as label-retaining cells after a chase period of 6 wk. In pilot studies, because of HCl pre-treatment required for BrdU immunohistochemistry, it proved difficult to simultaneously produce high-quality signals for SCs, capillaries, and BrdU. Thus we combined chromogenic and fluorescence revelation approaches on the same preparations as shown in Figure 1, H and I. Among 100 consecutive β-gal$^+$ SCs, 34 were BrdU-positive SCs. The mean distance separating SCs from capillaries was 2.5 ± 3.3 μm for BrdU-retaining SCs and 2.9 ± 3.3 μm for BrdU-negative SCs : 80 versus 74% of SCs were at <5 μm from capillaries, 10 versus 19% at 5–10 μm, and 10 versus 7% at >10 μm (NS). After one dose of notexin in a control animal subjected to the same BrdU exposure regime, the percentage of BrdU-positive SCs dropped to 8% in the injected TA muscle, suggesting that the signal diluted during cell division of the progeny of previously quiescent SCs. Thus, juxtavascular niches house quiescent SCs but also label nonretaining cells.

### SCs Are Juxtavascular But Physically Separated from ECs in Mammal Species

SC proximity to capillaries was similarly detected in other mammal species, including rats (Figure 2, A and B), dogs and humans (Figure 2, C–E). Electron microscopy routinely showed SCs separated from ECs by the respective basal laminae. Two distinct patterns were found: close cell body apposition or SCs projecting a cytoplasmic process toward EC from a more distal site (Figure 2, A and B). In human deltoid muscle, confocal microscopy of 30-μm-thick sections immunostained for SC markers (NCAM or MYF5) and either vWF, an EC marker, or collagen IV, allowed 3D reconstructions of 134 SCs. Even those SCs most closely associated with capillaries remained separated from ECs by a patent interstitial space in at least one plane of observation. Under this angle, SC-to-capillary distance was: <2 μm (53%), 2–5 μm (15%), 5–10 μm (10%), 10–20 μm (5%), and >20 μm (17%). A similar proximity was found at all ages from 24 to 73 y (n = 17, no correlation with age) and in all tested muscle groups (data not shown).

SCs Are More Frequently Associated with Capillaries than Myonuclei

We then determined whether the proximity of capillaries to any structure situated at the periphery of myofibers could be due to a chance event. We used large reconstructions of four normal human deltoid muscle cross sections to explore the overall distribution of 337 SCs, 2972 myonuclei, and 2796 capillaries, detected by immunostaining with nuclear counterstaining. We first determined whether spatial distribution deviates from randomness, a pattern corresponding to the Poisson distribution, toward either clustering, i.e., attraction of points, or regularity, a pattern characterized by a minimal inviolable distance between points. We used Ripley's K function (Ripley, 1988), a spatial point pattern analysis method that relies on systematic computation of the position of neighbors of each object present in the field by successive targeting. This method uniquely allows the formal demonstration of nonrandomness of a spatial distribution. It demonstrated both regularity due to interposition of myofibers between points and clustering of both SCs and myonuclei with capillaries unrelated to their peripheral position (see Supplementary Data). Highly different numbers of myonuclei and SCs precluded comparison of their respective proximity to capillaries by Kr analysis. Therefore, we used the quadrat test, with grid squares calibrated (21 μm diagonally) to enclose the largest clusters (18 μm) detected by Kr analysis. Cross-tabulation tables and Fisher's exact test allowed 2 by 2 comparisons of respective frequencies of colocalization with capillaries within the same square of SCs, myonuclei, and virtual sarcolemmal points randomly distributed at the periphery of fibers. The proportion of colocalization with capillaries was much higher for SCs than myonuclei (88 $\pm$ 6 vs. 54 $\pm$ 3%, p < 0.0001) and for myonuclei than virtual sarcolemmal points (54 $\pm$ 3 vs. 35 $\pm$ 3%, p < 0.003).

SC Numbers Linearly Correlate with Capillarization Independently from the Myofiber Type

In another morphometric approach, we determined the number of capillaries immediately adjacent to each myofiber in three normal human deltoid muscle samples (2332 myofibers). Histogram of myofiber capillarization frequency was close to Gaussian (Figure 2F). In each case, a majority of SCs (51, 66, and 67%) was associated with myofibers ringed by five or more capillaries, SC detection rate increased linearly
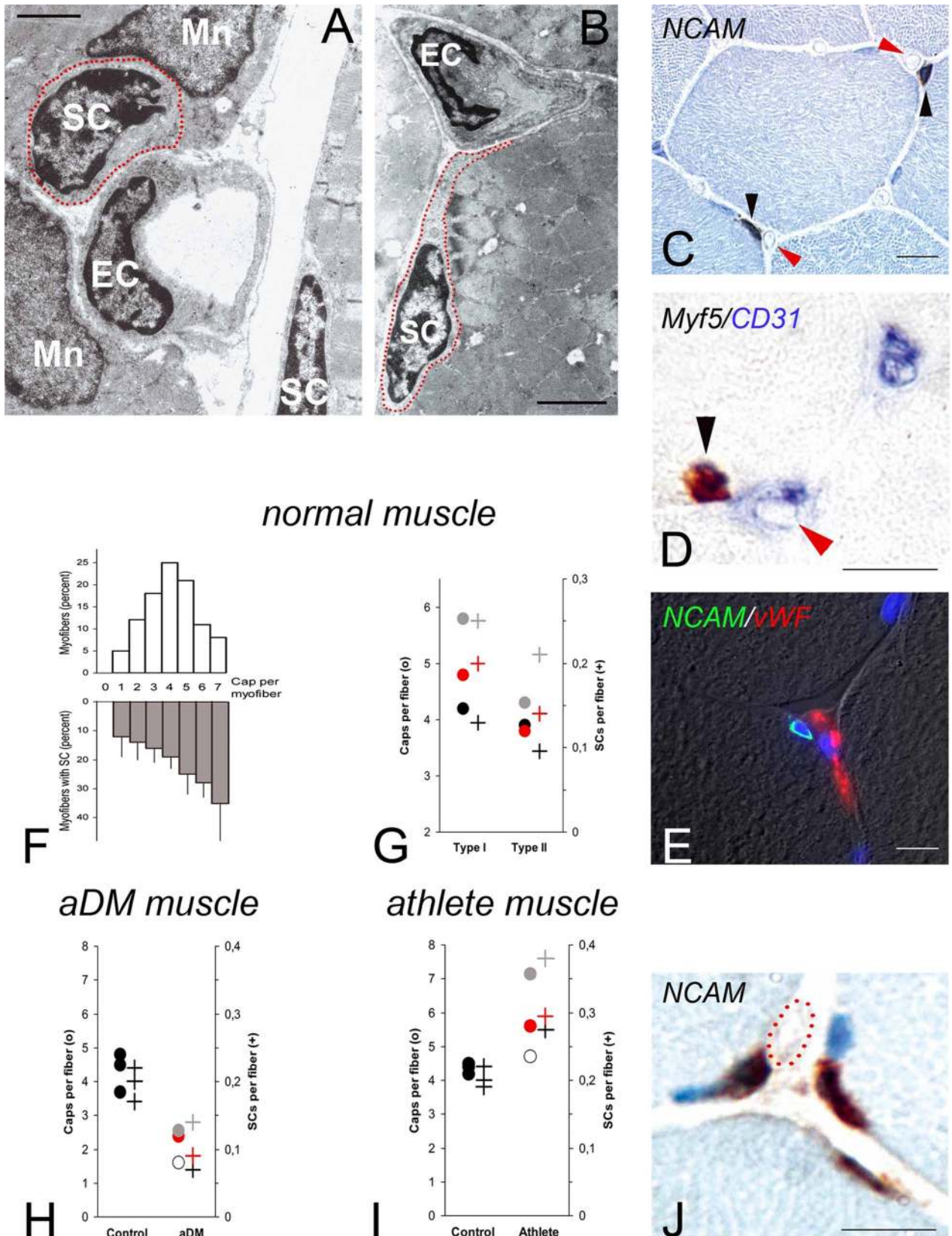
Figure 2. Topological relations between SCs and capillaries. (A and B) Transmission electron microscopy of rat SCs. Both apposition of SC body to EC (A) and apposition of a cytoplasmic process elongated from a distant SC toward EC (B) are observed. For clarity, SC plasma membrane was underlined by red dots. Please note the absence of direct SC-to-EC contact. Bars, 2 μm. (C–E) Chromogenic or fluorescent immunostainings of human deltoid muscle showing extreme proximity of SCs and capillaries. In C, SCs (black arrowheads) are immunostained for NCAM and capillaries (red arrowheads) are identified without immunostaining. In D, a SC nucleus is immunostained for Myf

with myofiber capillarization (χ^2 test for trend, p < 0.0001; Figure 2F).

Fast-myosin immunostaining was used to discriminate fast (type II) from slow (type I) muscle fibers. In each case, type II fibers had less surrounding capillaries than type I fibers (Figure 2G), the average capillarization being 3.6 ± 0.7 and 4.9 ± 0.8 per fiber, respectively (p < 0.0001). Type II fibers also showed a lower number of SCs, largely proportionate to their capillarization (Figure 2G).

Because of mosaicism of human muscle, a number of capillaries are shared by fibers of different types. Capillaries contacting type I, type II, or both type I and II fibers were similarly associated with SCs (range 2.4–5.2 vs. 2.4–5.8 vs. 2.8–6.0%, χ^2 test: NS in each case). Accordingly, capillaries contacting both type I and II fibers accounted for 67–78% of capillaries surrounding type II fibers and were associated with 63–77% of SCs in this fiber type. A similar correlation was found in type I myofibers (42–73 and 53–74%) pointing out capillarization as a plausible factor governing SC frequency in myofibers regardless of their type.

Muscle Capillary Loss Is Associated with Proportionate SC Decrease

As muscle blood vessels can proliferate or regress under the control of a variety of physiological and pathological stimuli (Emslie-Smith and Engel, 1990; Duscha et al., 1999; Jensen et al., 2004), we explored how SCs react to the reduction or increase of the microvascular bed. We deliberately chose situations in which microvascular changes occur without interfering pathological myofiber alterations.

We used aDM as a paradigm of pure capillary loss, typically observed in the absence of both myofiber damage and inflammation (Emslie-Smith and Engel, 1990; Cosnes et al., 1995). Compared with matched controls, three aDM patients selected from a previous study (Cosnes et al., 1995) had myofiber capillarization decreased by 45%, as previously reported (Emslie-Smith and Engel, 1990). Importantly a roughly proportionate decrease (53%) in the mean SC number per myofiber (Figure 2H) was also observed. Undepleted SCs remained strongly colocalized with capillaries (quadrat test: 91 ± 2% in aDM vs. 88 ± 6% in controls), indicating joint loss of SCs and capillaries in the same areas (Figure 2I).

Figure 2 (cont). 5 (black arrowhead) and capillaries (red arrowheads) are immunostained for CD31. (E) NCAM of SC plasma membrane is green, and the EC marker vWF is red. Bar, 10 μm. (F and G) Correlations between SCs and capillaries in normal muscle. Left graph (F), histogram of myofiber capillarization frequency (top) is close to Gaussian, whereas SC frequency (bottom) increases linearly with myofiber capillarization (data pooled from 3 normal deltoid muscles). Right graph (G), numbers of both capillaries (●) and SCs (+) are different and largely proportionate in type I and type II myofibers (individual results from 3 normal deltoid muscles identified by different colors). (H) Correlations between SCs and capillaries in aDM muscle. A proportionate loss of muscle capillaries (●) and SCs (+) was found in 3 patients with aDM (in red, gray, and white, respectively) compared with 3 age, sex, and muscle-matched normal controls (in black). (I and J) Heavy-trained muscle. (I) compared with their controls (in black), 3 athletes (in red, gray and white, respectively) show an increase of both muscle capillaries (●) and SCs (+). (J) SC clusters are formed by accumulations of SCs (NCAM+, brown) belonging to different myofibers, often adjacent to a myonucleus (hematoxylin nuclear counterstaining in blue) and surrounding the same capillary (red dots). Bar, 10 μm.

Capillary Increase Is Associated with Both SC Increase and Perivascular Accumulation in Trained Muscle

As workload is known to increase muscle capillary density (Carpenter and Karpati, 2001; Bischoff and Franzini-Armstrong, 2004; Jensen et al., 2004), we analyzed deltoid muscle samples from three heavy-training athletes. Athletes showed increased mean numbers of both capillaries (33%) and SCs (56%) per myofiber (Figure 2I). SCs remained close to capillaries (quadrat test: 87 ± 5%) where they often formed perivascular accumulations, appearing as pairs or triplets of SCs facing each other in adjacent myofibers (Figure 2J). Similar SC accumulations around vessels are routinely detected in pathological muscle biopsies showing repair or regeneration (data not shown). This prompted us to examine possible EC effects on myogenic cell proliferation, in vitro.

EC Monolayers Specifically Increase Myogenic Cell Growth through Soluble Factors

We further investigated EC interactions with myogenic cells, using cocultures under conditions avoiding cell–cell contacts between cell types. In vitro, SCs are released from quiescence and undergo exponential cell growth mimicking an injury model rather than the stable state of quiescent sublaminal SCs. In the same way, the standard EC monolayer culture is characterized by both inherent dedifferentiation of ECs and lack of contact with mural cells, i.e., pericytes and SMCs, that tightly control EC maturation (Korff et al., 2001). Therefore, EC monolayers mimic a situation of immature microvessels (Korff et al., 2001). These characteristics imply good relevance of EC–myogenic cell cocultures to dynamic states at work during muscle tissue formation and regeneration.

Human myogenic cells were plated in the lower chamber of culture wells, whereas the upper transwell compartment, separated by a porous filter, was seeded with HUVECs, human microvascular ECs (HMECs), human SMCs, human fibroblast cell line (MRC-5) or, as a control, other human myogenic precursor cells (mpc) derived from different primary cultures. mpc growth was strongly promoted in the presence of EC monolayers (Figure 3A). Compared with controls, both HUVECs and HMECs increased mpc growth, at day 3 (158%, p < 0.02; 227%, p < 0.008), day 5 (245%, p < 0.004; 203%, p < 0.003), and day 7 (259%, p < 0.0001; 212%, p = 0.0005). In contrast, no increase of mpc growth was observed with SMC or MRC-5 fibroblasts. These findings demonstrate that EC monolayers specifically release soluble factors that promote myogenic cell growth.

EC-derived IGF-1, HGF, bFGF, PDGF-BB, and VEGF Promote SC Growth

To detect the main EC-derived molecules increasing SC growth, we used both mRNA profiling by DNA macroarray to screen mpc expression of growth factor receptors and protein array to assess EC secretion of soluble effectors (see Materials and Methods). Of the 397 genes represented on our DNA macroarray membrane, 84 were receptors for soluble factors. Among them, receptors of five factors known to mediate mpc proliferation and survival signals were constitutively expressed by human mpc (Figure 3B). The protein array allowed detection of the corresponding ligands, including IGF-1, HGF, bFGF, PDGF-BB, and VEGF, in HUVEC-conditioned medium (Figure 3B).

Functional involvement of the detected molecules was assessed using specific blocking antibodies (Figure 3C). mpc were incubated for 3 d with antibodies deposited at saturat-

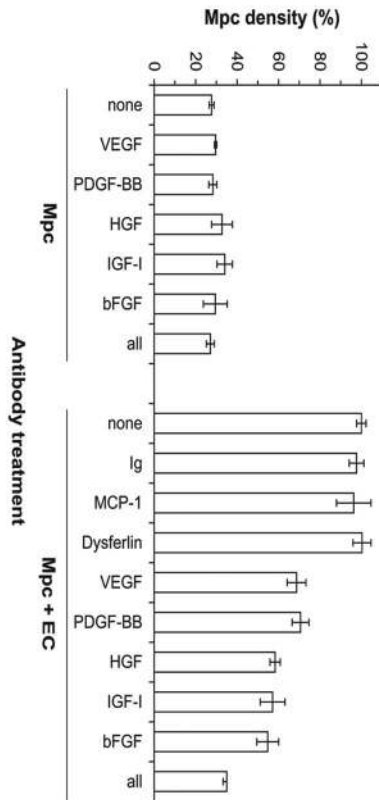## A - *in vitro mpc growth in presence of various cell types*
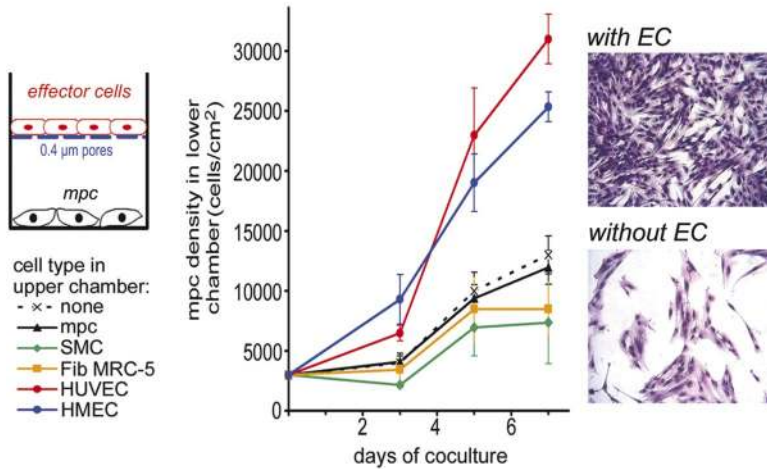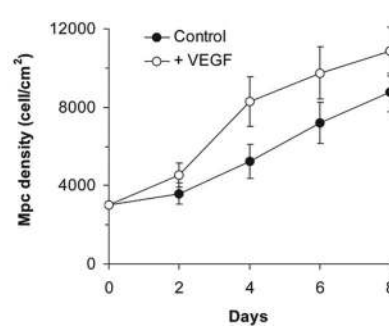

B - *selection of candidate effectors*

Gene expression by mpc

Gene name	Intensity
c-met	18
IGF-I R	189
PDGF Rb	221
PDGF Ra	450
FGF R1	193
FGF R3	94
FGF R2	42
Flk-1	36

Protein secretion by HUVEC

Protein name	Intensity
HGF	11
IGF-1	9
PDGF-BB	50
bFGF	71
VEGF	12

C - *effector inhibiton by blocking antibodies*


D - *effect of VEGF on mpc growth*

Figure 3. ECs stimulate SC growth. (A) In vitro mpc growth in presence of various cell types. Mpc cocultures were done using a bicameral insert avoiding direct cell–cell contacts between cell types. Coculture with either HUVECs or HMECs markedly increased mpc growth, whereas other cell types, including SMC, MRC-5 fibroblasts, or heterologous mpc, had no effect. Photos show representative mpc cultures with and without HUVECs at day 5 of coculture. (B) Selection of candidate effectors. DNA macroarray and protein array showed expression of 5 growth factor receptor mRNAs and their ligands by human mpc and HUVECs, respectively, assessed by signals above internal negative controls. Signal intensity is conventionally expressed in arbitrary densitometric units. (C) Functional involvement of the candidate effectors. Mpc grown alone and incubated with blocking antibodies against IGF-1, HGF, bFGF, PDGF-BB, and VEGF showed no significant change in their growth. In contrast, in cocultures, the same antibodies induced reduction of HUVEC-induced growth effect. This was not observed with nonrelevant antibodies (whole Igs, anti-MCP-1, or anti-Dysferlin antibodies) assessing implication of the five effectors in EC paracrine effects on mpc. (D) Incubation of mpc cultures with recombinant VEGF. Human mpc cultured with VEGF (25 ng/ml) showed significant enhancement of their growth compared with mpc cultured without VEGF ($p < 0.05$). Results are the mean $\pm$ SEM of 5 experiments run in duplicate.

ing concentrations in the lower chamber of the coculture insert. Although no changes in cell growth were detected when mpc were grown alone, significant effects of blocking antibodies were observed in cocultures. HUVEC-sustained mpc growth decreased by 41–62.5% after IGF-1, HGF, bFGF, PDGF-BB, and VEGF inhibition (all $p < 0.01$). Global inhibition obtained by pooling all five blocking antibodies resulted in a 90% inhibition of mpc growth ($p < 0.01$). Incubation with immunoglobulins or nonrelevant antibodies (MCP-1 and dysferlin) did not affect growth of mpc cocul-

tured with ECs. These results strongly implicate the five tested effectors in EC paracrine stimulation of mpc growth.

Unlike other effectors, VEGF has not been definitely demonstrated to directly stimulate muscle cell growth, although previous in vivo observations gave support for this view (Arsic *et al.*, 2004). Thus, we incubated mpc cultures with 25 ng/ml recombinant VEGF and measured cell density every 2 d. mpc growth increased at all evaluated time points (paired Student's *t* test: $p < 0.05$), the increase reaching 58% at day 4 (Figure 3D), thus confirming SC responsiveness to VEGF.
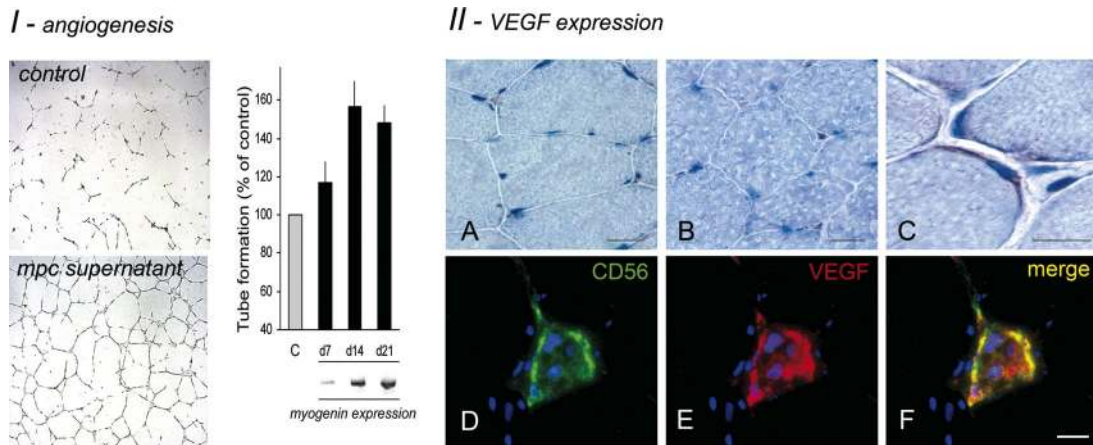
Figure 4. Myogenic cells are proangiogenic. (I) In vitro mpc proangiogenic activity. Compared with control (top), mpc (day 14) conditioned-medium (bottom) stimulated the formation of tubular-like structures by HUVECs in matrigel (24-h exposure, phase contrast). Proangiogenic activity significantly increased with mpc differentiation, assessed by Myogenin immunoblotting. (II) In vivo localization of VEGF. (A) Normal human muscle show weak microvascular immunostaining. (B) Amyopathic dermatomyositis shows virtually no signal. (C) Athlete muscle shows VEGF immunostaining in SCs with elongated processes. (D–F) Immunofluorescence shows a myofiber undergoing postnecrotic regeneration enclosing marginally located NCAM/CD56$^+$ myogenic cells (green) coexpressing VEGF (red). Bar, 5 μm (except C where magnification is about fourfold higher).

Differentiating Myogenic Cells Are Proangiogenic In Vitro

Resident cells of many tissues can signal to ECs and influence the angiogenic process (Cleaver and Melton, 2003). We examined if muscle cells do so, using primary cultures. Angiogenesis was assessed by measuring capillary-like structure formation of HUVECs plated on Matrigel (Jones *et al.*, 1999). A 24-h incubation of HUVECs with day 14 human mpc-conditioned medium increased the proportion of connected ECs by 169% (42.4 ± 13.2 in basal medium vs. 71.5 ± 8.7 in conditioned medium, p < 0.04) and the number of junctions between vascular tubes by 156% (10.5 ± 1.2 per field vs. 16.4 ± 1.4, p < 0.03). A proangiogenic effect of myogenic cells was observed from the proliferation stage (day 7), increased with differentiation, as assessed by expression of the late myogenic factor Myogenin, and culminated at the time of myoblast fusion into myotubes, i.e., at day 14 in our assay (day 7 vs. 14, p < 0.02; Figure 4, I).

This effect is in agreement with our previous observation that human mpc produce VEGF, the key angiogenic factor, during their differentiation (Chazaud *et al.*, 2003b). Therefore, we assayed for VEGF expression, in vivo (Figure 4, II). Normal human muscle showed no VEGF expression by SCs, but faint diffuse microvascular immunostaining (Figure 4A), as previously illustrated (Rissanen *et al.*, 2002). aDM muscle was almost completely negative (Figure 4B). In contrast, athlete muscles showed VEGF immunostaining in a small proportion of SCs with elongated processes suggestive of some degree of activation (Figure 4C). Consistently, VEGF was detected in NCAM/CD56$^+$ myogenic cells in routine muscle biopsies showing necrotic/regenerating fibers (Figure 4, D–F).

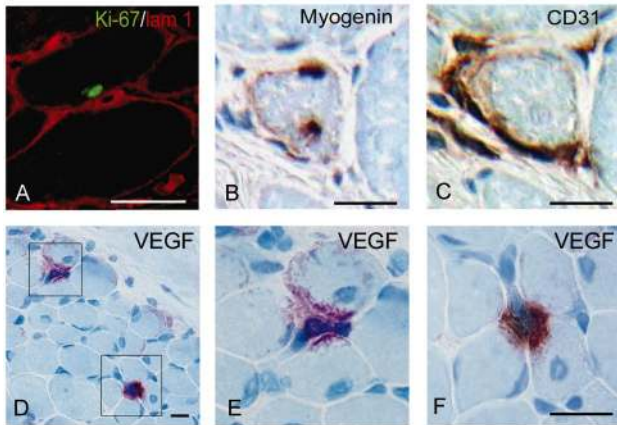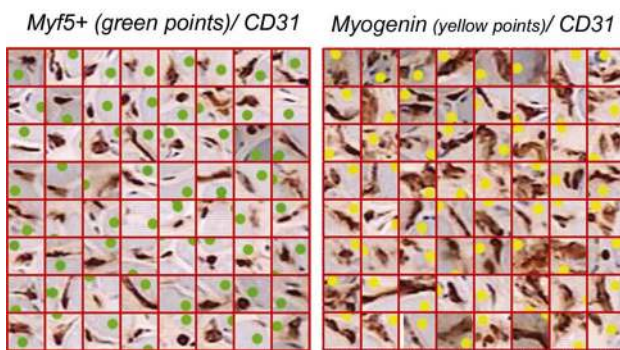### Myogenesis and Angiogenesis Are Spatiotemporally Correlated in DMD

To further investigate possible relationships between myofiber repair and angiogenesis, we analyzed muscle biopsies of three patients with DMD, a severe myopathy characterized by repeated cycles of intense myofiber degeneration/regeneration occurring in small clusters (Carpenter and Karpati, 2001).

We first immunolabeled the Ki-67 nuclear antigen which is associated with all cell proliferation phases but is absent in resting cells (G0). A maximum of 8% of NCAM/CD56$^+$ cells

were Ki-67$^+$ in DMD muscles. Double staining for Ki-67 and Laminin 1 showed that 82% of Ki-67$^+$ sublaminal SCs were colocalized with capillaries (Figure 5A). Ki-67 was occasionally detected in SC pairs. Thus, SCs does not need to leave their juxtavascular location to undergo active proliferation, and they can benefit from EC supportive cues in this position.

Moreover, myogenic cell differentiation assessed by Myogenin expression was associated with neoangiogenesis (Figure 5, B and C). DMD muscle cross sections contained a total number of 175 undifferentiated MYF5$^+$ SCs, and 211 Myogenin$^+$ cells undergoing myogenic differentiation. The quadrat test showed that 97.4% Myogenin$^+$ nuclei (vs. 88.5% MYF5$^+$ nuclei) colocalized with CD31$^+$ ECs. Moreover, the area occupied by ECs was about twofold higher in grid squares enclosing Myogenin$^+$ cells than in those enclosing MYF5$^+$ cells (48 ± 28 vs. 19 ± 18 μm², 59 ± 33 vs. 32 ± 18 μm², 44 ± 25 vs. 23 ± 18 μm²; all p < 0.0001; Figure 5, II). In addition, most capillaries associated with Myogenin$^+$ cells were sectioned longitudinally, indicating a tortuous and highly interconnected capillary network (Figure 5, II) typical of neoangiogenesis in skeletal muscle (Hansen-Smith *et al.*, 1996). These data reveal strong spatiotemporal correlation between myogenic cell differentiation and neoangiogenesis.

The multifocal pattern of angio-myogenesis was consistent with the distribution of VEGF immunostaining. In DMD, discrete foci of intense VEGF positivity were separated by nearly negative areas (Figure 5, D–F). It was difficult to unambiguously identify cell sources of VEGF in these foci, but the observed pattern was recently predicted by a computational model in which VEGF focally produced by muscle cells remains sequestered near sources of VEGF secretion bound to both VEGF receptors and heparan sulfate proteoglycans present at high concentrations in the muscle microenvironment (Mac Gabhann *et al.*, 2006). Centronucleation, the hallmark of in vivo muscle regeneration, was detected next to positive areas, and orientation of interstitial cells at this level was suggestive of angiogenic sprouts growing at nearly 90° from parent vessels against the steep VEGF gradient (Figure 5, D–F).

Figure 5. Combined myogenesis and angiogenesis in DMD. (I) Myogenesis and angiogenesis in DMD. (A) Double immunostaining for nuclear Ki-67 antigen (green) and laminin 1 (red) shows a sublaminal SC undergoing cell cycling close to a capillary. (B and C) Alternate sections immunostained for Myogenin and CD31, showing differentiating myogenic cells directly adjacent to transversely oriented neovessels. (D–F) VEGF immunostaining showing two discrete foci of intense positivity visualizing VEGF, sequestered next to myofibers with a central nucleus, directing transverse angiogenic sprouting. (II) Spatial association of myogenesis and angiogenesis in DMD. Selected squares enclosing both CD31^{+} ECs (brown) and either MYF5^{+} (green points) or myogenin^{+} (yellow points) cells from quadrat test applied to a DMD muscle. Myogenin^{+} cells undergoing late myogenic differentiation were associated with larger EC cytoplasmic areas than undifferentiated MYF5^{+}-positive SCs (these illustrations were built from alternate sections immunostained for MYF5, CD31, and Myogenin, myogenic cell positions being manually reported in the graphic plane of image reconstruction of CD31 immunostaining).

DISCUSSION

In the present report we show that SC niches are juxtavascular; that they can incorporate ectopic stem cells without loosing this anatomical characteristic; that most SCs remain in close proximity to capillaries regardless of their state of quiescence, proliferation and differentiation; and that individual myogenic cell differentiation is spatiotemporally associated with new vessel formation. In light of our in vitro experiments, these previously unappreciated morphological characteristics likely favor bidirectional signaling between ECs and differentiating SCs at work during muscle regeneration.

Factors that govern SC frequency are not known (Bischoff and Franzini-Armstrong, 2004). Although the frequency of SCs

appears to be much higher in slow compared with fast muscles (Zammit and Beauchamp, 2001), there is little difference at birth, and the metabolic properties per se may not be crucially involved (Bischoff and Franzini-Armstrong, 2004). Capillaries are more numerous in slow muscles than in fast ones (Hudlicka *et al.,* 2004). This may represent a key factor if one considers the linear increase of SCs with capillaries we observed at the individual myofiber level, regardless of the myofiber type. Notably, to avoid influence of the different workload of slow and fast individual muscles, a single type I–type II balanced muscle was chosen to compare fiber types. Conversely, in aDM, where focal capillary loss is insidious enough to cause no myofiber damage (Emslie-Smith and Engel, 1990), SC loss is proportionate to capillary loss and selectively affects capillary-depleted myofibers. Of note, this is not the case in full-blown dermatomyositis, where strong SC proliferation may be observed, despite marked capillary loss, in reaction to conspicuous ischemic myofiber damage and inflammation (Carpenter and Karpati, 2001). SCs are more resistant to acute ischemia than myonuclei (Snow, 1977; Schultz *et al.,* 1988), suggesting that disappearance of SCs in areas of capillary dropout in aDM may reflect, at least in part, loss of supportive paracrine EC signals. Investigating factors involved in SC maintenance and self-renewal would likely require complex assays integrating EC and myofiber-to-SC signaling. Detection of perivascular SC accumulations in trained muscle led us to examine the role of ECs in more dynamic states associated with SC proliferation. We used indirect EC–mpc coculture as an in vitro counterpart of muscle repair. EC monolayers that mimick immature capillaries supported mpc growth through release of soluble factors. Notably, mpc growth was not supported by fibroblasts and SMCs, two other cell types that may be found in the endomysium close to SCs. A direct role for paracrine signaling between ECs and surrounding target cells has been described during embryonic development and cell differentiation of several organs (Cleaver and Melton, 2003) but data in muscle are scant. Endothelial progenitors have been isolated from fetal tissues and adult blood (Le Grand *et al.,* 2004; De Angelis *et al.,* 1999; Shmelkov *et al.,* 2005) and can be instructed to codifferentiate into functional angiomyogenic colonies (Shmelkov *et al.,* 2005) and restore dystrophin in dystrophin-deficient mice and dogs (Le Grand *et al.,* 2004; Torrente *et al.,* 2004; Sampaolesi *et al.,* 2006). As shown here-in, circulating stem cells can incorporate juxtavascular SC niches of irradiated mice (LaBarge and Blau, 2002; Dreyfus *et al.,* 2004), but the physiological relevance of this phenomenon remains far from clear (Sherwood *et al.,* 2004). Nevertheless, vascular precursors enter the quail limb buds around the time of muscle precursors (Nimmagadda *et al.,* 2004), and vessels develop before the appearance of SCs in the mouse limb (Le Grand *et al.,* 2004). In wing buds of avian embryos, migrating myogenic cells may be found in close proximity to a prepatterned vascular network (Solursh *et al.,* 1987). In line with these observations, spatiotemporal correlations between the ingrowth of blood vessels into a formerly ischemic area and detection of cells with myogenic capacities in that area has been repeatedly reported (Phillips *et al.,* 1987; Kardon *et al.,* 2002). Although the lineage relationships between ECs and muscle progenitors is not firmly agreed upon in the literature, our present studies do strongly support a functional relationship.

Muscle regeneration after injury is associated with an increase in both capillarization and cross-sectional area of individual regenerating myofibers (Luque *et al.,* 1995). In the same way, most data on compensatory muscle hypertrophy due to overload reveal an almost linear relationship between capillary-to-fiber ratio and fiber area (Snow, 1977). Our anatomical and functional results indicate what cellular events

may underpin these structural changes. Human myogenic cells undergoing differentiation secrete VEGF (Chazaud *et al.*, 2003b). Conversely, we and others have shown that human ECs can produce a series of mitogens for myogenic cells (Hawke and Garry, 2001), and our coculture studies indicated that bFGF, IGF-1, HGF, VEGF, and PDGF-BB mediate the bulk of paracrine EC sustaining effect on mpc growth. Recently, attention has been paid to the role of VEGF and its receptors in muscle biology (Williams and Annex, 2004). Under normal in vivo conditions, mature ECs do not produce VEGF but express VEGF receptors R1 (Flt-1) and R2 (KDR/Flk-1), which may bind low-levels of VEGF uniformly released by normal muscle tissue (Mac Gabhann *et al.*, 2006). Exercise-induced VEGF up-regulation in muscle cells operate physiological angiogenesis (Egginton *et al.*, 2001; Ameln *et al.*, 2005). Myoblasts manipulated to produce VEGF specifically promote HUVEC proliferation (Kim *et al.*, 2006) and induce pronounced localized angiogenesis in their immediate vicinity after im transplantation (Springer *et al.*, 2003). A steep gradient of VEGF concentration emanating from the implantation site into neighboring host muscle tissue has been repeatedly predicted, but was not previously documented by immunolocalization (Springer *et al.*, 2003; Mac Gabhann *et al.*, 2006). It was visualized herein in DMD, possibly because VEGF release occurs at a particularly high rate in dystrophin deficient tissue (Nico *et al.*, 2002).

VEGF receptor expression is not restricted to ECs and VEGF effects extend to a variety of nonendothelial cell types, including myogenic cells (Rissanen *et al.*, 2002, Germani *et al.*, 2003, Motoike *et al.*, 2003, Arsic *et al.*, 2004). We showed that VEGF stimulates in vitro myogenic cell growth. In addition, VEGF stimulates their migration (Germani *et al.*, 2003), protects them from apoptosis (Germani *et al.*, 2003, Arsic *et al.*, 2004), up-regulate myoglobin expression (van Weel *et al.*, 2004), and promotes formation of centronucleated myofibers (Arsic *et al.*, 2004).

On these grounds, evidence that, upon activation, SCs accumulate and proliferate close to capillaries, receive efficient support from ECs for their growth, are proangiogenic, and colocalize with new vessel formation during their myogenic differentiation, strongly suggests that angiogenesis and myogenesis reciprocally signal. It is likely that angiogenesis and myogenesis share VEGF as a coregulatory factor (Williams and Annex, 2004) probably in combination with other factors known to stimulate both ECs and SCs, such as bFGF or IGF1 (Bischoff and Franzini-Armstrong, 2004; Hawke and Garry, 2001). We assume that, following workload or more pronounced injury, angiogenesis is tightly coordinated with SC proliferation, differentiation, and fusion to underlying myofibers. Newly SC-derived myonuclei may remain close to capillaries, as suggested by the frequent colocalization of myonuclei with capillaries. Occasional observation of SCs immediately adjacent to a myonucleus (Figure 2J) is even reminiscent of the model proposed by Moss and Leblond (1971) in which assymetrical SC division generates a new SC and a daughter cell fated to become a myonucleus. Newly incorporated myonuclei likely produce muscle-specific proteins causing increase of the myofiber cross-section size. Harmonious increase of myofiber capillarization and caliber ensues, allowing larger myofibers to benefit from an appropriately enhanced blood supply.

Such a myo-vascular unit may share similarities with the vascular neural stem cell niche that supports intimate combination of neurogenesis and angiogenesis in the brain (Palmer *et al.*, 2000; Shen *et al.*, 2004).

The knowledge that muscle SCs evolve into a juxtavascular niche may be critical for several reasons. It provides a novel clue to investigate poorly understood muscle patho-logical processes combining capillary bed and myofiber size variations (Emslie-Smith and Engel, 1990; Duscha *et al.*, 1999; Hudlicka *et al.*, 2004; Jensen *et al.*, 2004). Moreover, it could pave the way for improved myoblast transfer therapy of heart, sphincter, and skeletal muscle diseases. Dramatic non-mechanic transplanted cell death is a major limitation of this therapeutic approach (Chazaud *et al.*, 2003a). The present results suggest that early cell death results from extrinsic growth factor deprivation of mpc massively implanted in an inappropriate microanatomic environment (Chazaud *et al.*, 2003b). Recreating an appropriate endothelial cell or molecular support to the transplanted stem cells thus represents a promising way to improve striated muscle cell therapies.

ACKNOWLEDGMENTS

REFERENCES

Ameln, H., Gustafsson, T., Sundberg, C. J., Okamoto, K., Jansson, E., Poellinger, L., and Makino, Y. (2005). Physiological activation of hypoxia inducible factor-1 in human skeletal muscle. FASEB J. *19*, 1009–1011.

Asakura, A., Komaki, M., and Rudnicki, M. (2001). Muscle satellite cells are multipotential stem cells that exhibit myogenic, osteogenic, and adipogenic differentiation. Differentiation *68*, 245–253.

Arsic, N., Zacchigna, S., Zentilin, L., Ramirez-Correa, G., Pattarini, L., Salvi, A., Sinagra, G., and Giacca, M. (2004). Vascular endothelial growth factor stimulates skeletal muscle regeneration in vivo. Mol. Ther. *10*, 844–854.

Beauchamp, J. R., Heslop, L., Yu, D. S., Tajbakhsh, S., Kelly, R. G., Wernig, A., Buckingham, M. E., Partridge, T. A., and Zammit, P. S. (2000). Expression of CD34 and myf5 defines the majority of quiescent adult skeletal muscle satellite cells. J. Cell Biol. *151*, 1221–1234.

Bischoff, R., and Franzini-Armstrong, C. (2004). Satellite and stem cells in muscle regeneration. In: Myology, ed. A. G. Engel and C. Franzini-Armstrong, New-York: McGraw Hill, 66–86.

Carpenter, S., and Karpati, G. (2001). Pathology of Skeletal Muscle, New York: Oxford University Press.

Chazaud, B. *et al.* (2003a). Endoventricular porcine autologous myoblast transplantation can be successfully achieved with minor mechanical cell damage. Cardiovasc. Res. *58*, 444–450.

Chazaud, B., Sonnet, C., Lafuste, P., Bassez, G., Rimaniol, A. C., Poron, F., Authier, F. J., Dreyfus, P. A., and Gherardi, R. K. (2003b). Satellite cells attract monocytes and use macrophages as a support to escape apoptosis and enhance muscle growth. J. Cell Biol. *163*, 1133–1143.

Chretien, F., Dreyfus, P. A., Christov, C., Caramelle, P., Lagrange, J. L., Chazaud, B., and Gherardi, R. K. (2005). In vivo fusion of circulating fluorescent cells with dystrophin-deficient myofibers results in extensive sarcoplasmic fluorescence expression but limited dystrophin sarcolemmal expression. Am. J. Pathol. *166*, 1741–1748.

Cleaver, O., and Melton, D. A. (2003). Endothelial signaling during development. Nat. Med. *9*, 661–668.

Collins, C. A., Olsen, I., Zammit, P. S., Heslop, L., Petrie, A., Partridge, T. A., and Morgan, J. E. (2005). Stem cell function, self-renewal, and behavioral heterogeneity of cells from the adult muscle satellite cell niche. Cell *122*, 289–301.

Cosnes, A., Amaudric, F., Gherardi, R., Verroust, J., Wechsler, J., Revuz, J., and Roujeau, J. C. (1995). Dermatomyositis without muscle weakness. Long-term follow-up of 12 patients without systemic corticosteroids. Arch. Dermatol. *131*, 1381–1385.

De Angelis, L., Berghella, L., Coletta, M., Lattanzi, L., Zanchi, M., Cusella-De Angelis, M. G., Ponzetto, C., and Cossu, G. (1999). Skeletal myogenic progenitors originating from embryonic dorsal aorta coexpress endothelial and myogenic markers and contribute to postnatal muscle growth and regeneration. J. Cell Biol. *147*, 869–878.

Dhawan, J., and Rando, T. A. (2005). Stem cells in postnatal myogenesis: molecular mechanisms of satellite cell quiescence, activation and replenishment. Trends Cell Biol. *15*, 666–673.

Dreyfus, P. A., Chretien, F., Chazaud, B., Kirova, Y., Caramelle, P., Garcia, L., Butler-Browne, G., and Gherardi, R. K. (2004). Adult bone marrow-derived

stem cells in muscle connective tissue and satellite cell niches. Am. J. Pathol. *164*, 773–779.

Duscha, B. D., Kraus, W. E., Keteyian, S. J., Sullivan, M. J., Green, H. J., Schachat, F. H., Pippen, A. M., Brawner, C. A., Blank, J. M., and Annex, B. H. (1999). Capillary density of skeletal muscle: a contributing mechanism for exercise intolerance in class II-III chronic heart failure independent of other peripheral alterations. J. Am. Coll. Cardiol. *33*, 1956–1963.

Egginton, S., Zhou, A. L., Brown, M. D., and Hudlicka, O. (2001). Unorthodox angiogenesis in skeletal muscle. Cardiovasc. Res. *49*, 634–646.

Emslie-Smith, A. M., and Engel, A. G. (1990). Microvascular changes in early and advanced dermatomyositis: a quantitative study. Ann. Neurol. *27*, 343–356.

Fuchs, E., Tumbar, T., and Guasch, G. (2004). Socializing with the neighbors: stem cells and their niche. Cell *116*, 769–778.

Germani, A., Di Carlo, A., Mangoni, A., Straino, S., Giacinti, C., Turrini, P., Biglioli, P., and Capogrossi, M. C. (2003). Vascular endothelial growth factor modulates skeletal myoblast function. Am. J. Pathol. *163*, 1417–1428.

Gros, J., Manceau, M., Thome, V., and Marcelle, C. (2005). A common somitic origin for embryonic muscle progenitors and satellite cells. Nature *435*, 954–958.

Hansen-Smith, F. M., Hudlicka, O., and Egginton, S. (1996). In vivo angiogenesis in adult rat skeletal muscle: early changes in capillary network architecture and ultrastructure. Cell Tissue Res. *286*, 123–136.

Hawke, T. J., and Garry, D. J. (2001). Myogenic satellite cells: physiology to molecular biology. J. Appl. Physiol. *91*, 534–551.

Hudlicka, O., Brown, M. D., and Egginton, S. (2004). Microcirculation in muscle. In: Myology, ed A. G. Engel, C. Franzini-Armstrong, New York: McGraw Hill, 511–533.

Jensen, L., Bangsbo, J., and Hellsten, Y. (2004). Effect of high intensity training on capillarisation and presence of angiogenic factors in human skeletal muscle. J. Physiol. *557*, 571–582.

Jones, M. K., Wang, H., Peskar, B. M., Levin, E., Itani, R. M., Sarfeh, I. J., and Tarnawski, A. S. (1999). Inhibition of angiogenesis by nonsteroidal anti-inflammatory drugs: insight into mechanisms and implications for cancer growth and ulcer healing. Nat. Med. *5*, 1418–1423.

Kardon, G., Campbell, J. K., and Tabin, C. J. (2002). Local extrinsic signals determine muscle and endothelial cell fate and patterning in the vertebrate limb. Dev. Cell *3*, 533–545.

Kassar-Duchossoy, L., Gayraud-Morel, B., Gomes, D., Rocancourt, D., Buckingham, M., Shinin, V., and Tajbakhsh, S. (2004). Mrf 4 determines skeletal muscle identity in Myf5, MyoD double-mutant mice. Nature *431*, 466–470.

Kim, K. I. *et al.* (2006). β-catenin overexpression augments angiogenesis and skeletal muscle regeneration through dual mechanism of vascular endothelial growth factor–mediated endothelial cell proliferation and progenitor cell mobilization. Arterioscler. Thromb. Vasc. Biol. *26*, 91–98.

Korff, T., Kimmina, S., Martiny-Baron, G., and Augustin, H. G. (2001). Blood vessel maturation in a 3-dimensional spheroidal coculture model: direct contact with smooth muscle cells regulates endothelial cell quiescence and abrogates VEGF responsiveness. FASEB J. *15*, 447–457.

LaBarge, M. A., and Blau, H. M. (2002). Biological progression from adult bone marrow to mononucleate muscle stem cell to multinucleate muscle fiber in response to injury. Cell *111*, 589–601.

Le Grand, F., Auda-Boucher, G., Levitsky, D., Rouaud, T., Fontaine-Perus, J., and Gardahaut, M. F. (2004). Endothelial cells within embryonic skeletal muscles: a potential source of myogenic progenitors. Exp. Cell Res. *301*, 232–241.

Li, L., and Xie, T. (2005). Stem cell niche: structure and function. Annu. Rev. Cell Dev. Biol. *21*, 605–631.

Luque, E., Pena, J., Martin, P., Jimena, I., and Vaamonde, R. (1995). Capillary supply during development of individual regenerating muscle fibers. Anat. Histol. Embryol. *24*, 87–89.

Mac Gabhann, F., Ji, J. W., and Popel, A. S. (2006). Computational model of vascular endothelial growth factor spatial distribution in muscle and pro-angiogenic cell therapy. PLoS Comput. Biol. *2*, e127. Epub 2006 Aug 3.

Maurer, M. H., Tripps, W. K., Feldmann, R. E., Jr., and Kuschinsky, W. (2003). Expression of vascular endothelial growth factor and its receptors in rat neural stem cells. Neurosci. Lett. *344*, 165–168.

Mauro, A. (1961). Satellite cell of skeletal muscle fibers. J. Biophys. Biochem. Cytol. *9*, 493–495.

Motoike, T., Markham, D. W., Rossant, J., and Sato, T. N. (2003). Evidence for novel fate of Flk1+ progenitor: contribution to muscle lineage. Genesis *35*, 153–159.

Molnar, G., Ho, M. L., and Schroedl, N. A. (1996). Evidence for multiple satellite cell populations and a non-myogenic cell type that is regulated differently in regenerating and growing skeletal muscle. Tissue Cell *28*, 547–556.

Moss, F. P., and Leblond, C. P. (1971). Satellite cells as the source of nuclei in muscles of growing rats. Anat. Rec. *170*, 421–435.

Nico, B., Corsi, P., Vacca, A., Roncali, L., and Ribatti, D. (2002). Vascular endothelial growth factor and vascular endothelial growth factor receptor-2 expression in *mdx* mouse brain. Brain Res. *953*, 12–16.

Nimmagadda, S., Loganathan, P. G., Wilting, J., Christ, B., and Huang, R. (2004). Expression pattern of VEGFR-2 (Quek1) during quail development. Anat. Embryol. *208*, 219–224.

Okabe, M., Ikawa, M., Kominami, K., Nakanishi, T., and Nishimune, Y. (1997). 'Green mice' as a source of ubiquitous green cells. FEBS Lett. *407*, 313–319.

Palmer, T. D., Willhoite, A. R., and Gage, F. H. (2000). Vascular niche for adult hippocampal neurogenesis. J. Comp. Neurol. *425*, 479–494.

Pearce, S. S., Hudlick, O., and Brown, M. D. (2000). Effect of indomethacin on capillary growth and microvasculature in chronically stimulated rat skeletal muscles. J. Physiol. *526*, 435–443.

Phillips, G. D., Lu, D. Y., Mitashov, V. I., and Carlson, B. M. (1987). Survival of myogenic cells in freely grafted rat rectus femoris and extensor digitorum longus muscles. Am. J. Anat. *180*, 365–372.

Ripley, B. D. (1988). Statistical Inference for Spatial Processes, Cambridge: Cambridge University Press.

Rissanen, T. T. *et al.* (2002). Expression of vascular endothelial growth factor and vascular endothelial growth factor receptor-2 (KDR/Flk-1) in ischemic skeletal muscle and its regeneration. Am. J. Pathol. *19*, 1393–1403.

Rouger, K., Brault, M., Daval, N., Leroux, I., Guigand, L., Lesoeur, J., Fernandez, B., and Cherel, Y. (2004). Muscle satellite cell heterogeneity: in vitro and in vivo evidences for populations that fuse differently. Cell Tissue Res. *317*, 319–326.

Sampaolesi, M. *et al.* (2006). Mesoangioblast stem cells ameliorate muscle function in dystrophic dogs. Nature *444*, 574–579.

Schmalbruch, H., and Hellhammer, U. (1977). The number of nuclei in adult rat muscles with special reference to satellite cells. Anat. Rec. *189*, 169–175.

Schultz, E., and Lipton, B. H. (1982). Skeletal muscle satellite cells: changes in proliferation potential as a function of age. Mech. Ageing Dev. *20*, 377–383.

Schultz, E., Albright, D. J., Jaryszak, D. L., and David, T. L. (1988). Survival of satellite cells in whole muscle transplants. Anat. Rec. *222*, 12–17.

Seale, P., Sabourin, L. A., Girgis-Gabardo, A., Mansouri, A., Gruss, P., and Rudnicki, M. A. (2000). Pax7 is required for the specification of myogenic satellite cells. Cell *102*, 777–786.

Shen, Q., Goderie, S. K., Jin, L., Karanth, N., Sun, Y., Abramova, N., Vincent, P., Pumiglia, K., and Temple, S. (2004). Endothelial cells stimulate self-renewal and expand neurogenesis of neural stem cells. Science *304*, 1338–1340.

Sherwood, R. I., Christensen, J. L., Conboy, I. M., Conboy, M. J., Rando, T. A., Weissman, I. L., and Wagers, A. J. (2004). Isolation of adult mouse myogenic progenitors: functional heterogeneity of cells within and engrafting skeletal muscle. Cell *19*, 543–554.

Shinin, V., Gayraud-Morel, B., Gomes, D., and Tajbakhsh, S. (2006). Asymmetric division and cosegregation of template DNA strands in adult muscle satellite cells. Nat. Cell Biol. *8*, 677–687.

Shmelkov, S. V. *et al.* (2005). Cytokine preconditioning promotes codifferentiation of human fetal liver CD133+ stem cells into angiomyogenic tissue. Circulation *111*, 1175–1183.

Snow, M. H. (1977). Myogenic cell formation in regenerating rat skeletal muscle injured by mincing. II. An autoradiographic study. Anat. Rec. *188*, 201–217.

Solursh, M., Drake, C., and Meier, S. (1987). The migration of myogenic cells from the somites at the wing level in avian embryos. Dev. Biol. *121*, 389–396.

Sonnet, C., Lafuste, P., Arnold, L., Brigitte, M., Poron, F., Authier, F. J., Chretien, F., Gherardi, R. K., and Chazaud, B. (2006). Human macrophages rescue myoblasts and myotubes from apoptosis through a set of adhesion molecular systems. J. Cell Sci. *119*, 2497–2507.

Springer, M. L., Ozawa, C. R., Banfi, A., Kraft, P. E., Ip, T. K. Brazelton, T. R., and Blau, H. M. (2003). Localized arteriole formation directly adjacent to the site of VEGF-induced angiogenesis in muscle. Mol. Ther. *7*, 441–449.

Suda, T., Arai, F., and Hirao, A. (2005). Hematopoietic stem cells and their niche. Trends Immunol. *26*, 426–433.

Tajbakhsh, S., Bober, E., Babinet, C., Pournin, S., Arnold, H., and Buckingham, M. (1996). Gene targeting the myf-5 locus with nlacZ reveals expression of this

myogenic factor in mature skeletal muscle fibres as well as early embryonic muscle. Dev. Dynam. *206*, 291–300.

Tamaki, T., Akatsuka, A., Ando, K., Nakamura, Y., Matsuzawa, H., Hotta, T., Roy, R. R., and Edgerton, V. R. (2002). Identification of myogenic-endothelial progenitor cells in the interstitial spaces of skeletal muscle. J. Cell Biol. *157*, 571–577.

Tamaki, T., Uchiyama, Y., Okada, Y., Ishikawa, T., Sato, M., Akatsuka, A., and Asahara, T. (2005). Functional recovery of damaged skeletal muscle through synchronized vasculogenesis, myogenesis, and neurogenesis by muscle-derived stem cells. Circulation *112*, 2857–2866.

Tordjman, R., Delaire, S., Plouet, J., Ting, S., Gaulard, P., Fichelson, S., Romeo, P. H., and Lemarchandel, V. (2001). Erythroblasts are a source of angiogenic factors. Blood *97*, 1968–1974.

Torrente, Y. *et al.* (2004). Human circulating AC133(+) stem cells restore dystrophin expression and ameliorate function in dystrophic skeletal muscle. J. Clin. Invest. *114*, 182–195.

van Weel, V., Deckers, M.M.L., Grimbergen, J.M., van Leuven, K.J.M., Lardenoye, J.H.P., Schlingemann, R. O., van Nieuw Amerongen, G. P., van Bockel, J. H., van Hinsbergh, V.W.M., and Quax, P.H.A. (2004). Vascular endothelial growth factor overexpression in ischemic skeletal muscle enhances myoglobin expression in vivo. Circ. Res. *95*, 58–66.

Williams, R. S. and Annex, B. H. (2004). Plasticity of myocytes and capillaries: a possible coordinating role for VEGF. Circ. Res. *95*, 7–8.

Zammit, P., and Beauchamp, J. (2001). The skeletal muscle satellite cell: stem cell or son of stem cell? Differentiation *68*, 193–204.